Ab initio study of parity and time-reversal violation in laser-coolable triatomic molecules

Konstantin Gaul and Robert Berger*
Fachbereich Chemie, Philipps-Universität Marburg, Hans-Meerwein-Straße 4, 35032 Marburg, Germany

(Received 4 July 2019; published 13 January 2020)

Electronic structure enhancement factors of simultaneous parity and time-reversal violation ($\mathcal{P},\mathcal{T}$ violation) caused by an electric dipole moment of the electron (eEDM) and scalar-pseudoscalar nucleon-electron current (SPNEC) interactions are reported for various metal monohydroxides, several of which are considered laser-coolable and promising candidates for an eEDM measurement. Electronic structure enhancements are calculated *ab initio* within zeroth-order regular approximation (ZORA) for CaOH, SrOH, BaOH, RaOH, and YbOH. Scaling behavior with respect to nuclear charge numbers and the ratio of enhancement factors for both discussed sources of $\mathcal{P},\mathcal{T}$ violation are analyzed, which are crucial to obtaining stringent bounds on parameters for new physics from experiments.

DOI: 10.1103/PhysRevA.101.012508

I. INTRODUCTION

High-precision spectroscopy of diatomic molecules serves as a powerful tool for probing high-energy scales of new physics beyond the standard model of particle physics [1]. Signatures of new physics are expected for instance from simultaneous parity $\mathcal{P}$ and time-reversal $\mathcal{T}$ violation [2]. Such a violation of fundamental symmetries can in principle result in a permanent electric dipole moment of a molecule in a vanishing electric field. With cold polar heavy molecules such as ThO, currently the strictest limits are set on $\mathcal{P},\mathcal{T}$-violating effects due to the electric dipole moment of the electron (eEDM) [3,4]. This is due to electronic structure effects in polar heavy diatomic molecules, which strongly enhance $\mathcal{P},\mathcal{T}$-odd effects such as an eEDM d_e or scalar-pseudoscalar nucleon-electron current (SPNEC) interactions [5]. References [6–8] highlighted the particular situation of $\mathcal{P},\mathcal{T}$-odd effects in the diatomic system RaF, which was earlier identified to have the advantage of being also a molecular candidate for laser cooling [9]. Based on simple theoretical concepts [10] (for a review see [11]) it was subsequently concluded that not only diatomic, but also polyatomic molecules can be cooled with lasers. This renders such molecules promising laboratories for the study of fundamental symmetry violations. A number of molecular candidates were proposed [10] which included the particular example of CaOH. The first successful experiment of laser cooling of a polyatomic molecule was subsequently realized with SrOH [12]. Isaev *et al.* [13] suggested laser cooling of RaOH and its use to search for new physics. They presented also the first calculation of SPNEC interactions enhancement in a polyatomic molecule.

Kozyryev *et al.* elucidated that laser-coolable polyatomic molecules, and in particular YbOH, can have advantages over diatomic molecules in experimental setups and may improve sensitivity of eEDM experiments [14]. And it was pointed out in Ref. [15] that diatomic molecules are limited in the sensitivity of a simultaneous determination of d_e as well as the coupling constant of SPNEC interactions k_s when one analyzes the scaling behavior of the enhancement factors with respect to the charge of the heavy nucleus.

To provide these enhancement factors for upcoming experiments on triatomic molecules, we present in this paper predictions of W_d and W_s, the electronic structure enhancement factors of an eEDM and SPNEC interactions, respectively, in the laser-coolable polyatomic molecules CaOH, SrOH, RaOH, and YbOH, as well as for BaOH, which is isoelectronic to BaF, a promising candidate for the first detection of molecular parity violation [16]. We compare herein also the ratio W_d/W_s to those obtained for diatomic molecules in order to gauge the advantage of polyatomic over diatomic molecules with respect to electronic structure enhancement effects.

II. THEORY

A. $\mathcal{P},\mathcal{T}$-odd spin-rotational Hamiltonian of a linear molecule

The metal hydroxides (MOH) studied herein are linear molecules and expected to have a $^2\Sigma_{1/2}$ ground state. Thus the effective $\mathcal{P},\mathcal{T}$-odd spin-rotational Hamiltonian (see review [17]) when neglecting contributions of the light nuclei and nuclear spin-dependent effects is the same as for diatomic molecules studied in Ref. [15], namely,

$$H_{sr} = (k_s W_s + d_e W_d)\Omega, \tag{1}$$

where $\Omega = \vec{J}_e \cdot \vec{\lambda}$ is the projection of the reduced total electronic angular momentum $\vec{J}_e$ on the molecular axis, defined by the unit vector $\vec{\lambda}$ pointing from the heavy nucleus to the OH group. k_s is the $\mathcal{P},\mathcal{T}$-odd scalar-pseudoscalar nucleon-electron current interaction constant and d_e is the eEDM. The complete $\mathcal{P},\mathcal{T}$-odd spin-rotational operator, including nuclear spin-dependent terms, we discuss elsewhere [18]. The $\mathcal{P},\mathcal{T}$-odd electronic structure parameters are defined by

$$W_s = \frac{\langle\Psi|\hat{H}_s|\Psi\rangle}{k_s\Omega} \quad \text{and} \quad W_d = \frac{\langle\Psi|\hat{H}_d|\Psi\rangle}{d_e\Omega}, \tag{2}$$

*Corresponding author: robert.berger@uni-marburg.de

where Ψ is the electronic wave function. The molecular $\mathcal{P}, \mathcal{T}$-odd Hamiltonians [2,19,20]

$$\hat{H}_\mathrm{s} = \imath k_\mathrm{s} \frac{G_\mathrm{F}}{\sqrt{2}} \sum_{i=1}^{N_\mathrm{elec}} \sum_{A=1}^{N_\mathrm{nuc}} \rho_A(\vec{r}_i) Z_A \boldsymbol{\gamma}^0 \boldsymbol{\gamma}^5, \tag{3}$$

$$\hat{H}_\mathrm{d} = \frac{2\imath c d_\mathrm{e}}{\hbar e} \sum_{i=1}^{N_\mathrm{elec}} \boldsymbol{\gamma}^0 \boldsymbol{\gamma}^5 \hat{\vec{p}}_i^2 \tag{4}$$

were implemented and evaluated in a quasirelativistic framework within the zeroth-order regular approximation (ZORA) [15,21]:

$$\hat{H}_\mathrm{s}^\mathrm{ZORA} = \imath \sum_{i=1}^{N_\mathrm{elec}} \sum_{A=1}^{N_\mathrm{nuc}} Z_A [\rho_A(\vec{r}_i) \tilde{\omega}_\mathrm{s}(\vec{r}_i), \vec{\boldsymbol{\sigma}} \cdot \hat{\vec{p}}_i]_-, \tag{5}$$

$$\hat{H}_\mathrm{d}^\mathrm{ZORA} = \imath \sum_{i=1}^{N_\mathrm{elec}} \hat{\vec{p}}_i^2 \tilde{\omega}_\mathrm{d}(\vec{r}_i)(\vec{\boldsymbol{\sigma}} \cdot \hat{\vec{p}}_i) - (\vec{\boldsymbol{\sigma}} \cdot \hat{\vec{p}}_i) \tilde{\omega}_\mathrm{d}(\vec{r}_i) \hat{\vec{p}}_i^2. \tag{6}$$

Here ρ_A is the normalized nuclear charge density distribution of nucleus A with charge number Z_A, $\vec{r}_i$ is the position vector of electron i, $G_\mathrm{F} = 2.22249 \times 10^{-14}\ E_\mathrm{h} a_0^3$ is Fermi's weak coupling constant, $\imath = \sqrt{-1}$ is the imaginary unit, $\hat{\vec{p}}$ is the linear momentum operator, $\vec{\boldsymbol{\sigma}}$ is the vector of the Pauli spin matrices, $[A, B]_- = AB - BA$ is the commutator, and the modified ZORA factors are defined as

$$\tilde{\omega}_\mathrm{s}(\vec{r}_i) = \frac{G_\mathrm{F} k_\mathrm{s} c}{\sqrt{2}(2m_\mathrm{e}c^2 - \tilde{V}(\vec{r}_i))}, \tag{7}$$

$$\tilde{\omega}_\mathrm{d}(\vec{r}_i) = \frac{2 d_\mathrm{e} c^2}{2e\hbar m_\mathrm{e} c^2 - e\hbar \tilde{V}(\vec{r}_i)}, \tag{8}$$

with the model potential $\tilde{V}$ introduced by van Wüllen [22], which is used to alleviate the gauge dependence of ZORA. Here c is the speed of light in vacuum, $\hbar = \frac{h}{2\pi}$ is the reduced Planck constant, and m_e is the mass of the electron.

B. Calculation of hyperfine coupling constants within cGHF and cGKS

Hyperfine coupling constants were evaluated starting from the relativistic electronic hyperfine operator of nucleus A:

$$\hat{H}_\mathrm{hf} = \sum_i \vec{\boldsymbol{\alpha}} \cdot \vec{\mu}_A \times \frac{(\vec{r}_i - \vec{r}_A)}{|\vec{r}_i - \vec{r}_A|^3}, \tag{9}$$

with the nuclear magnetic moment $\vec{\mu}_A$. The effective spin-rotation Hamiltonian of hyperfine couplings appears as

$$\hat{H}_\mathrm{sr,hf} = \vec{I}_A \cdot \mathbf{A} \cdot \vec{S}, \tag{10}$$

where $\mathbf{A}$ is the hyperfine tensor, and $\vec{I}_A$ and $\vec{S}$ are the effective nuclear and electron spin, respectively. In a linear molecule with the molecular axis being aligned on the z axis we have

$$\hat{H}_\mathrm{sr,hf} = I_{z,A} S_z A_\parallel + (I_{x,A} S_x + I_{y,A} S_y) A_\perp. \tag{11}$$

In our complex generalized Hartree-Fock/complex generalized Kohn-Sham (cGHF/cGKS) approach, which accounts for spin polarization, the molecular orbitals are not necessarily obtained as Kramers pairs. The zz component of the hyperfine tensor is thus calculated by

$$A_{zz} = -\frac{\mu_A}{2cm_\mathrm{p} I_A S_z} \left\langle \sum_i \frac{[(\vec{r}_i - \vec{r}_A) \times \vec{\boldsymbol{\alpha}}]_z}{|\vec{r}_i - \vec{r}_A|^3} \right\rangle. \tag{12}$$

Here μ_A is the nuclear magnetic moment in units of μ_N, I_A is the nuclear spin quantum number and $\langle \hat{O} \rangle$ is the expectation value of operator $\hat{O}$ computed for the cGHF or cGKS determinant. Therefore, the $A_\parallel$ component was calculated from A_{zz} [Eq. (12)] by alignment of the molecular axis and the electronic spin on the z axis, whereas the $A_\perp$ component was received from the A_{zz} for the wave function with the molecular axis aligned on the x axis but the electronic spin aligned on the z axis.

III. COMPUTATIONAL DETAILS

The quasirelativistic two-component calculations reported herein are performed within ZORA at the level of complex generalized Hartree-Fock (cGHF) or Kohn-Sham (cGKS) with a modified version [23–26] of the quantum chemistry program package TURBOMOLE [27]. For details on our implementation of $\mathcal{P}, \mathcal{T}$-odd properties within this ZORA framework see Refs. [15,21,28]. For Kohn-Sham (KS) density functional theory (DFT) calculations, the hybrid Becke three-parameter exchange functional and Lee, Yang, and Parr correlation functional (B3LYP) [29–32] were employed.

For all calculations a basis set of $37s$, $34p$, $14d$, and $9f$ uncontracted Gaussian functions with the exponential coefficients α_i composed as an even-tempered series as $\alpha_i = ab^{N-i}$; $i = 1, \ldots, N$, with $b = 2$ for s and p functions and with $b = (5/2)^{1/25} \times 10^{2/5} \approx 2.6$ for d and f functions was used for the electropositive atom. The largest exponent coefficients of the s, p, d and f subsets are $2 \times 10^9\ a_0^{-2}$, $5 \times 10^8\ a_0^{-2}$, $13300.758\ a_0^{-2}$ and $751.8368350\ a_0^{-2}$, respectively. The O atoms were represented with a decontracted s, p, d substratum of the atomic natural orbital (ANO) basis set of triple-ζ quality for F [33] and for H the s, p subsets of a decontracted correlation-consistent basis of quadruple-ζ quality [34] was used.

The ZORA-model potential $\tilde{V}(\vec{r})$ was employed with additional damping [35] as proposed by van Wüllen [22]. For two-component wave functions and properties a finite nucleus was used, described by a normalized spherical Gaussian nuclear density distribution $\rho_A(\vec{r}) = \rho_0\, e^{-\frac{3}{2\zeta_A}\vec{r}^2}$. The rms radius ζ_A of nucleus A was used as suggested by Visscher and Dyall [36], where the mass numbers A are ^{43}Ca, ^{87}Sr, ^{137}Ba, ^{173}Yb, ^{223}Ra.

The nuclear equilibrium distances were obtained at the levels of GHF-ZORA and GKS-ZORA/B3LYP, respectively. For calculations of energy gradients at the DFT level the nucleus was approximated as a point charge. The molecular structure parameters obtained are summarized in Table I.

IV. RESULTS

Our results for W_d and W_s are presented together with angular momentum quantum numbers Ω in Table II. All Ω values are close to the expected value $1/2$. Minor numerical deviations from $1/2$ are due to an imperfect alignment of the total electronic spin and angular momentum on the molecular

TABLE I. Molecular structure parameters calculated within a quasirelativistic ZORA approach at the cGHF and cGKS/B3LYP levels for metal hydroxide radicals MOH with M = Ca, Sr, Ba, Ra, Yb.

	$r(M\text{-O})$ (Å)		r(O-H) (Å)		$\sphericalangle(M\text{-O-H})$ (deg)	
M	cGHF	cGKS	cGHF	cGKS	cGHF	cGKS
Ca	2.006	1.972	0.932	0.954	179.91	179.70
Sr	2.134	2.110	0.933	0.955	179.99	179.93
Ba	2.239	2.207	0.935	0.956	179.93	179.95
Ra	2.315	2.289	0.935	0.956	179.93	179.93
Yb	2.083	2.002	0.933	0.953	179.92	179.92

axis, which cannot always be enforced within the cGHF or cGKS approach.

Values calculated for W_d and W_s on the DFT level for group 2 hydroxides differ only slightly from those obtained with GHF, which is in agreement with previous studies of $\mathcal{P},\mathcal{T}$ violation in group 2 compounds [15]. The larger deviation for YbOH hints that electron correlation effects are more important for this f-block compound. However, previous comparisons of our method with four-component coupled-cluster calculations for corresponding metal fluoride molecules show that the accuracy of the present approach can be estimated to be on the order of about 20% (see Ref. [21]), which is fully sufficient for the present purpose.

We find that compared to $\mathcal{P},\mathcal{T}$-odd enhancement in metal fluorides, calculated in Ref. [15], the values for the corresponding hydroxides are slightly larger in magnitude, but all in all differences are very small, below 5%. Considering possible improvements of the experimental setup with polyatomic molecules as described in Ref. [14], experiments with laser-coolable RaOH or YbOH as promising candidates for an improvement of current limits on the eEDM consequently would benefit mainly from full polarization of the molecule and the existence of internal co-magnetometer states, but not from improved electronic enhancement factors. The potential of the latter in polyatomic molecules is thus yet to be explored.

The proposed eEDM measurements in polyatomic molecules are planned to be performed in the first vibrational excited state [14] of the electronic ground state. However, vibrational corrections to the $\mathcal{P},\mathcal{T}$-odd properties presented herein are expected to be on the order of <10% and, thus, are below the predicted precision of our calculations. Furthermore, the first vibrational excited states in MOH compounds are the degenerate H-O bending modes υ_2, which do not affect the M-O bonding much. For example, a rough estimate of vibrational corrections in the first vibrational state of YbOH was calculated from the potential energy surface (PES) within ZORA-cGHF (see Fig. 1). In leading order, vibrational corrections to the isotropic part of W_d for the H-O

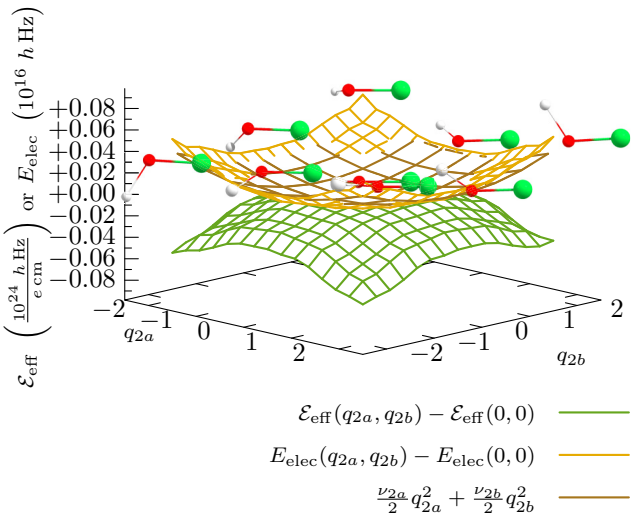

FIG. 1. Potential energy surface (PES) of YbOH in the space of the Yb-O-H bending mode q_{2a} and q_{2b} (lowest lying vibrational modes) with respect to the energy of the equilibrium structure at $q_{2a}=0$, $q_{2b}=0$: $E_\mathrm{elec}(q_{2a},q_{2b})-E_\mathrm{elec}(0,0)$ (yellow [light gray] plane), compared to the pure harmonic PES of YbOH (brown [dark gray] plane). The harmonic PES is determined from the harmonic vibrational wave number $\tilde{\nu}_{2a}=321$ cm^{-1} and $\tilde{\nu}_{2b}=347$ cm^{-1} corresponding to q_{2a} and q_{2b}, respectively. The degeneracy of the harmonic wave numbers is thus slightly lifted due to numerical reasons. The change of the effective internal electrical field that enhances the eEDM $\mathcal{E}_\mathrm{eff}=\Omega W_\mathrm{d}$ at the equilibrium structure is shown in dependency of q_{2a} and q_{2b} as well (green [medium gray] plane). All data were obtained at the level of ZORA-cGHF with a large even-tempered basis set. The equilibrium structure and displaced structures of YbOH for $q_{2a},q_{2b}=-2.2,0,2.2$ are shown. Elements are represented as Yb (big, green [medium gray]), O (medium, red [dark gray]), and H (small, light grey).

TABLE II. Projection of the reduced total electronic angular momentum on the molecular axis and $\mathcal{P},\mathcal{T}$-violating properties of hydroxide radicals calculated *ab initio* within a quasirelativistic two-component ZORA approach at the cGHF and cGKS/B3LYP level. Dev. refers to the relative deviation between cGHF and cGKS results.

		Ω[a]		W_s (h Hz)			W_d ($10^{24}\,\frac{h\,\mathrm{Hz}}{e\,\mathrm{cm}}$)		
Molecule	Z	cGHF	cGKS	cGHF	cGKS	Dev.	cGHF	cGKS	Dev.
CaOH	20	−0.494	−0.499	-2.18×10^{2}	-2.14×10^{2}	2%	-1.44×10^{-1}	-1.41×10^{-1}	2%
SrOH	38	−0.500	−0.500	-2.00×10^{3}	-1.97×10^{3}	1%	−1.04	−1.03	1%
BaOH	56	0.483	0.483	-8.79×10^{3}	-7.91×10^{3}	10%	−3.32	−2.98	10%
RaOH	88	0.494	0.471	-1.53×10^{5}	-1.41×10^{5}	8%	-2.75×10^{1}	-2.53×10^{1}	8%
YbOH	70	−0.500	−0.495	-4.12×10^{4}	-3.08×10^{4}	25%	-1.14×10^{1}	−8.54	25%

[a]The absolute sign of Ω is arbitrary. However, relative to the sign of the effective electric field $W_\mathrm{d}\Omega$ it is always such that $\mathrm{sgn}(W_\mathrm{d})=-1$.

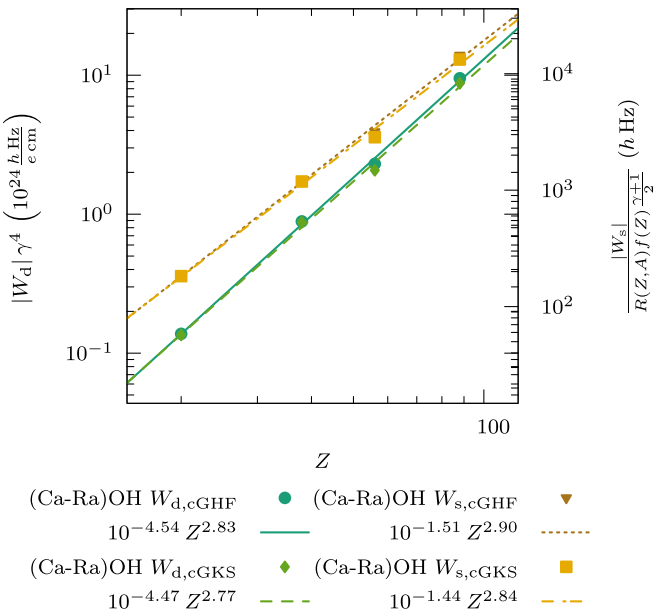

FIG. 2. Scaling of $\log_{10}\{|W_d|\gamma^4 \times 10^{-24}\,\frac{e\,\mathrm{cm}}{h\,\mathrm{Hz}}\}$ and $\log_{10}\{\frac{|W_s|}{R(Z,A)f(Z)^{\frac{\gamma+1}{2}}} \times \frac{1}{h\mathrm{Hz}}\}$ with $\log_{10}\{Z\}$ for group 2 hydroxides (Ca-Ra)OH at the level of GKS-ZORA/B3LYP and GHF-ZORA.

bending modes can be determined from

$$\langle \Psi, v_2 = 1|\hat{H}_d|\Psi, v_2 = 1\rangle \sim \frac{3}{8}\left(\frac{\partial^2\langle\Psi|\hat{H}_d|\Psi\rangle}{\partial q_{2a}^2} + \frac{\partial^2\langle\Psi|\hat{H}_d|\Psi\rangle}{\partial q_{2b}^2}\right), \quad (13)$$

where q_{2a} and q_{2b} are the dimensionless reduced normal coordinates of the degenerate O-H bending modes. The derivatives were evaluated numerically from the points of the PES. Our calculation predicts vibrational corrections on eEDM enhancement of $9 \times 10^{21}\,\frac{h\,\mathrm{Hz}}{e\,\mathrm{cm}}$, which is much less than 1% of W_d of YbOH and therefore far below the predicted accuracy of the present calculations. This is negligible as long as no eEDM has been measured. If one were led to use vibrational levels in higher lying electronic states as measurement states, computational methods for the description of electronically excited states would have to be used instead.

For further insight the scaling with nuclear charge Z is studied. For this purpose nonpolynomial relativistic enhancement is separated as described in Ref. [15] using relativistic enhancement factors known from atomic considerations [37–39]: $R_s = R(Z,A)f(Z)^{\frac{\gamma+1}{2}}$ and $R_d = \frac{1}{\gamma^4}$ with $f(Z) = \frac{1-0.56\alpha^2Z^2}{(1-0.283\alpha^2Z^2)^2}$ and $R(Z,A) = \frac{4}{\Gamma^2(2\gamma+1)}(2Zr_{nuc}/a_0)^{2\gamma-2}$. Here $\gamma = [(j+1/2)^2 - (\alpha Z)^2]^{1/2}$, j is the total electronic angular momentum quantum number, α is the fine structure constant, a_0 is the Bohr radius and $r_{nuc} \approx 1.2\ \mathrm{fm}\,A^{1/3}$. A double logarithmic plot for reduced cGHF and cGKS results as a function of Z together with a linear fit is presented in Fig. 2. The Z dependence for W_s (cGKS) of $Z^{2.83}$ is similar to that reported for group 2 fluorides in Ref. [15] for W_s (cGKS) of $Z^{2.79}$, whereas W_d scales steeper for MOH ($Z^{2.77}$) than for group 2 fluorides (Ref. [15]: $Z^{2.57}$).

In measurements of permanent molecular EDMs, various possible sources can be discussed and thus for robust bounds on $\mathcal{P},\mathcal{T}$-odd parameters, as the eEDM or k_s, complementary experiments have to be found, which are performed on systems with different electronic enhancement of the parameters. As discussed in detail in Ref. [15] the ratio W_d/W_s of two different experiments determines if the experiments are complementary or redundant for a parallel determination of k_s and d_e. In Table III the ratios W_d/W_s are compared to those of corresponding fluorides determined in Ref. [15].

TABLE III. $\mathcal{P},\mathcal{T}$-odd ratios W_d/W_s of hydroxide radicals MOH calculated within a quasirelativistic two-component ZORA approach at the cGKS/B3LYP level in comparison to ratios of corresponding fluoride radicals MF calculated in Ref. [15].

	W_d/W_s $(\frac{10^{20}}{e\,\mathrm{cm}})$	
M	MOH	MF
Ca	6.60	6.62
Sr	5.22	5.17
Ba	3.77	3.78
Ra	1.79	1.79
Yb	2.77	2.76

The values show that the metal hydroxides fit perfectly in the model developed in Ref. [15]. Hence there is in terms of electronic enhancement factors no immediate advantage of using a metal hydroxide instead of a fluoride. With respect to the coverage region in the parameter space of k_s and d_e, however, an experiment with MOH would be able to reduce the size of the coverage region due to the expected smaller systematic experimental uncertainties because of the presence of comagnetometer states. Experiments with the corresponding MF compounds could become redundant as essentially the same information regarding k_s and d_e is obtained.

As hyperfine coupling constants are sensitive to the behavior of s and p orbitals close to the nucleus, as well, and are directly measurable, we provide the parallel $A_\parallel$ and perpendicular components $A_\perp$ of the hyperfine coupling tensor calculated at the level of cGKS- and cGHF-ZORA in Table IV. $A_\parallel$ and $A_\perp$ can help to roughly estimate the error of the predicted $\mathcal{P},\mathcal{T}$-odd enhancement factors with respect to experiment, once microwave spectra of the proposed metal hydroxides containing high-spin isotopes of metal atoms are measured.

V. CONCLUSION

In this paper we reported the calculation of enhancements of an electric dipole moment of the electron in simple polyatomic molecules. Our calculations show that there is no considerable difference for enhancement factors between fluorides and hydroxides. This is also true for the ratio W_d/W_s. Thus, from a perspective of electronic enhancement factors there is no advantage in the use of MOH alongside MF in experiments as both experiments yield the same information on the parameter space of d_e and k_s. In order to see distinct differences from diatomic molecules it may be necessary to study more complex and nonlinear polyatomic molecules. However, together with the experimental benefits of polyatomic molecules described in Ref. [14] the herein studied molecules are promising candidates for an improvement of current limits on $\mathcal{P},\mathcal{T}$-violating effects.

TABLE IV. Hyperfine coupling constants calculated within a quasirelativistic ZORA approach at the cGHF and cGKS/B3LYP level for radical metal hydroxides MOH with $M = {}^{43}$Ca, ^{87}Sr, ^{137}Ba, ^{223}Ra, ^{173}Yb. Nuclear spins and nuclear magnetic moments are taken from Refs. [42,43].

			$A_\parallel$ (MHz)		$A_\perp$ (MHz)	
M	I_M	μ_M (μ_N)	cGHF	cGKS	cGHF	cGKS
^{43}Ca	$^7/_2$	−1.317 27	-3.6×10^2	-4.4×10^2	-3.4×10^2	-4.3×10^2
^{87}Sr	$^9/_2$	−1.092 83	-4.5×10^2	-5.8×10^2	-4.3×10^2	-5.6×10^2
^{137}Ba	$^3/_2$	0.937 365	1.9×10^3	2.3×10^3	1.8×10^3	2.3×10^3
^{223}Ra	$^3/_2$	0.2703	1.8×10^3	2.1×10^3	1.7×10^3	2.0×10^3
^{173}Yb	$^5/_2$	−0.67989	-1.6×10^3	-1.3×10^3	-1.6×10^3	–[a]

[a]The $^2\Sigma_{1/2}$ state of YbOH with total electronic spin aligned on the z axis and the molecular axis aligned on the x axis could not be converged within cGKS.

Note added. Recently, two other studies on $\mathcal{P},\mathcal{T}$-odd effects in YbOH and BaOH [40] and YbOH [41] were published. In Ref. [40] the results of our present paper are discussed and good agreement (relative deviations smaller than 7%) of the cGHF values has been found in comparison to their values obtained on the coupled-cluster level. As Dirac-Hartree-Fock results in Ref. [40] were obtained on the paired GHF level only, their values show larger discrepancy with coupled-cluster results due to the lack of spin-polarization effects. The coupled-cluster results for the effective electric field $\mathcal{E}_{\text{eff}}$ presented in Ref. [41] for linear structures of YbOH are also in good agreement (relative deviation less than 1%) with values at the level of cGHF.

ACKNOWLEDGMENTS

We thank Timur Isaev for inspiring discussions. Computer time provided by the Center for Scientific Computing (CSC) Frankfurt is gratefully acknowledged.

[1] D. DeMille, Phys. Today **68**(12), 34 (2015).
[2] I. B. Khriplovich and S. K. Lamoreaux, *CP Violation without Strangeness* (Springer, Berlin, 1997).
[3] J. Baron, W. C. Campbell, D. DeMille, J. M. Doyle, G. Gabrielse, Y. V. Gurevich, P. W. Hess, N. R. Hutzler, E. Kirilov, I. Kozyryev, B. R. O'Leary, C. D. Panda, M. F. Parsons, E. S. Petrik, B. Spaun, A. C. Vutha, and A. D. West, Science **343**, 269 (2014).
[4] V. Andreev, D. G. Ang, D. DeMille, J. M. Doyle, G. Gabrielse, J. Haefner, N. R. Hutzler, Z. Lasner, C. Meisenhelder, B. R. O'Leary, C. D. Panda, A. D. West, E. P. West, X. Wu, and A.C.M.E. Collaboration, Nature **562**, 355 (2018).
[5] J. S. M. Ginges and V. V. Flambaum, Phys. Rep. **397**, 63 (2004).
[6] T. A. Isaev and R. Berger, arXiv:1302.5682.
[7] A. D. Kudashov, A. N. Petrov, L. V. Skripnikov, N. S. Mosyagin, T. A. Isaev, R. Berger, and A. V. Titov, Phys. Rev. A **90**, 052513 (2014).
[8] S. Sasmal, H. Pathak, M. K. Nayak, N. Vaval, and S. Pal, Phys. Rev. A **93**, 062506 (2016).
[9] T. A. Isaev, S. Hoekstra, and R. Berger, Phys. Rev. A **82**, 052521 (2010).
[10] T. A. Isaev and R. Berger, Phys. Rev. Lett. **116**, 063006 (2016).
[11] T. A. Isaev and R. Berger, CHIMIA Int. J. Chem. **72**, 375 (2018).
[12] I. Kozyryev, L. Baum, K. Matsuda, B. L. Augenbraun, L. Anderegg, A. P. Sedlack, and J. M. Doyle, Phys. Rev. Lett. **118**, 173201 (2017).
[13] T. A. Isaev, A. V. Zaitsevskii, and E. Eliav, J. Phys. B **50**, 225101 (2017).
[14] I. Kozyryev and N. R. Hutzler, Phys. Rev. Lett. **119**, 133002 (2017).
[15] K. Gaul, S. Marquardt, T. Isaev, and R. Berger, Phys. Rev. A **99**, 032509 (2019).
[16] E. Altuntaş, J. Ammon, S. B. Cahn, and D. DeMille, Phys. Rev. Lett. **120**, 142501 (2018).
[17] M. G. Kozlov and L. N. Labzowsky, J. Phys. B **28**, 1933 (1995).
[18] K. Gaul and R. Berger, arXiv:1907.10432 [J. Chem. Phys. (to be published)].
[19] E. Salpeter, Phys. Rev. **112**, 1642 (1958).
[20] A. Mårtensson-Pendrill and P. Öster, Phys. Scr. **36**, 444 (1987).
[21] K. Gaul and R. Berger, J. Chem. Phys. **147**, 014109 (2017).
[22] C. van Wüllen, J. Chem. Phys. **109**, 392 (1998).
[23] R. Berger, N. Langermann, and C. van Wüllen, Phys. Rev. A **71**, 042105 (2005).
[24] R. Berger and C. van Wüllen, J. Chem. Phys. **122**, 134316 (2005).
[25] S. Nahrwold and R. Berger, J. Chem. Phys. **130**, 214101 (2009).
[26] C. van Wüllen, Z. Phys. Chem. **224**, 413 (2010).
[27] R. Ahlrichs, M. Bär, M. Häser, H. Horn, and C. Kölmel, Chem. Phys. Lett. **162**, 165 (1989).
[28] T. A. Isaev and R. Berger, Phys. Rev. A **86**, 062515 (2012).
[29] P. J. Stephens, F. J. Devlin, C. F. Chabalowski, and M. J. Frisch, J. Phys. Chem. **98**, 11623 (1994).
[30] S. H. Vosko, L. Wilk, and M. Nuisar, Can. J. Phys. **58**, 1200 (1980).
[31] A. D. Becke, Phys. Rev. A **38**, 3098 (1988).

[32] C. Lee, W. Yang, and R. G. Parr, Phys. Rev. B **37**, 785 (1988).
[33] B. O. Roos, R. Lindh, P. k. Malmqvist, V. Veryazov, and P. O. Widmark, J. Phys. Chem. A **108**, 2851 (2004).
[34] T. H. Dunning, Jr., J. Chem. Phys. **90**, 1007 (1989).
[35] W. Liu, C. van Wüllen, F. Wang, and L. Li, J. Chem. Phys. **116**, 3626 (2002).
[36] L. Visscher and K. G. Dyall, At. Data Nucl. Data Tables **67**, 207 (1997).
[37] V. A. Dzuba, V. V. Flambaum, and C. Harabati, Phys. Rev. A **84**, 052108 (2011).
[38] E. Fermi and E. Segrè, Mem. Acad. Ital. **4**, 131 (1933).
[39] E. Fermi and E. Segrè, Z. Phys. **82**, 729 (1933).
[40] M. Denis, P. A. B. Haase, R. G. E. Timmermans, E. Eliav, N. R. Hutzler, and A. Borschevsky, Phys. Rev. A **99**, 042512 (2019).
[41] V. S. Prasannaa, N. Shitara, A. Sakurai, M. Abe, and B. P. Das, Phys. Rev. A **99**, 062502 (2019).
[42] I. Mills, T. Cvitas, K. Homann, N. Kallay, and K. Kuchitsu, *Quantities, Units and Symbols in Physical Chemistry* (Blackwell Science, Oxford, 1988).
[43] K. M. Lynch, S. G. Wilkins, J. Billowes, C. L. Binnersley, M. L. Bissell, K. Chrysalidis, T. E. Cocolios, T. Goodacre, R. P. de Groote, G. J. Farooq-Smith, D. V. Fedorov, V. N. Fedosseev, K. T. Flanagan, S. Franchoo, R. F. Garcia Ruiz, W. Gins, R. Heinke, Á. Koszorús, B. A. Marsh, P. L. Molkanov *et al.*, Phys. Rev. C **97**, 024309 (2018).